



Oxidation of C_3H_8 , iso- C_5H_{12} and C_3H_6 under near-stoichiometric and fuel-lean conditions over aged Pt–Pd/ Al_2O_3 catalysts with different Pt:Pd ratios

Jonghyun Kim^{a,1}, Yongwoo Kim^{a,1}, Michelle H. Wiebenga^b, Se H. Oh^b, Do Heui Kim^{a,*}

^a School of Chemical and Biological Engineering, Institute of Chemical Processes, Seoul National University, Seoul 08826, Republic of Korea

^b General Motors Global R&D, 30500 Mound Road, Warren, MI 48090, USA

ARTICLE INFO

Keywords:

Hydrocarbon oxidation

Pt–Pd

Fully lean condition

Near-stoichiometric condition

Lean-rich cycling

ABSTRACT

Effective control of hydrocarbon (HC) emissions at low temperatures is critical for emission compliance, since a large fraction (typically 70–80%) of tailpipe HC emissions occurs during the first couple of minutes after an engine cold-start. The oxidation of propane, iso-pentane and propylene was investigated over Pd-only, Pt-only and Pt–Pd catalysts aged under lean-rich cycling conditions. Various characterizations such as XRD, XANES, STEM, CO chemisorption and H_2 -TPR were performed over the initial catalysts. Moreover, before and after the reaction, the states of the catalysts were characterized by XRD, XANES and STEM. The oxidation activity tests were carried out under both near-stoichiometric and fully lean conditions in the feedstream containing HC, O_2 , CO, H_2 , NO and H_2O . Under the near-stoichiometric condition, the Pt/ Al_2O_3 catalyst showed much higher activity for propane oxidation than the Pd/ Al_2O_3 and Pt–Pd/ Al_2O_3 catalysts. For propylene oxidation, on the other hand, the Pd/ Al_2O_3 catalyst was the most active, and the Pt/ Al_2O_3 catalyst exhibited the lowest activity due to the fact that the co-presence of CO and propylene on the Pt surface leads to their competition for a limited amount of adsorbed oxygen. Under the fully lean condition, metallic Pd in the Pd/ Al_2O_3 catalyst was gradually oxidized to PdO and consequently poisoned by H_2O , whereas there was little change in the state of the Pt/ Al_2O_3 catalyst, indicating higher stability of metallic Pt than Pd. However, a drastic decrease in the propane oxidation activity was observed over Pt/ Al_2O_3 in the presence of excess oxygen in the fully lean feed since preferential adsorption of oxygen on the Pt surface inhibited propane adsorption and thus the oxidation reaction. In addition, the propylene oxidation activity under the fully lean condition was greatly enhanced over all three catalysts compared to that observed under the near-stoichiometric condition, with Pd/ Al_2O_3 still being more active than Pt/ Al_2O_3 . The catalyst activity for iso-pentane oxidation was affected only to a relatively small extent by the high oxygen concentration, so that the same activity order among the catalysts (Pt > Pt–Pd > Pd) was observed under both the slightly lean and fully lean conditions. These results indicate that both hydrocarbon type and oxygen concentration level are important factors determining the relative oxidation activities of the various noble metal catalysts. Relatively small beneficial effects of Pt–Pd alloying were observed during iso-pentane oxidation at low temperatures under the near-stoichiometric conditions and during propane oxidation at high temperatures under the fully lean condition. However, alloy formation was found to be detrimental for the propane oxidation under the slightly lean condition.

1. Introduction

The catalytic removal of pollutants from vehicle exhaust gas has proven to be an effective means of meeting the ever-tightening emission standards since the introduction of catalytic converters in the middle of the 1970s [1]. However, future emission control technologies face considerable additional challenges and need further improvement because stricter emission standards must be met in the future while at the

same time complying with aggressive fuel economy regulation. The adoption of fuel-saving technologies (such as lean burn, turbocharging and advanced combustion) generally leads to considerably lower exhaust gas temperatures than those of conventional engines [2,3], thus posing significant challenges for low-temperature performance of emission control catalysts. Hence, it is critically important to understand and improve the performance characteristics of current commercial catalysts at low temperatures under realistic feedstream

* Corresponding author.

E-mail address: dohkim@snu.ac.kr (D.H. Kim).

¹ These authors contributed equally to this work.

<https://doi.org/10.1016/j.apcatb.2019.04.001>

Received 27 December 2018; Received in revised form 7 March 2019; Accepted 1 April 2019

Available online 02 April 2019

0926-3373/© 2019 Elsevier B.V. All rights reserved.

conditions.

Effective control of hydrocarbon (HC) emissions at low temperatures is critical for emission compliance since a large fraction (typically 70–80%) of tailpipe HC emissions occurs during the first couple of minutes after an engine cold-start. Gasoline engine exhaust contains a variety of HC species, including olefins, paraffins and aromatics [4,5]. The olefins in engine exhaust are unsaturated HCs in the C1–C3 range which represent incomplete combustion products. The paraffins in exhaust, which include unburned fuel, consist of saturated HCs with straight chains (n-alkanes) as well as those with a branched structure (alkane isomers).

Both Pd and Pt are generally known to be active for catalytic oxidation of various HCs. Pd is the active metal of choice for light HC combustion while Pt is more active for the oxidation of heavier HCs [6–8]. In addition, synergy between Pt and Pd has received considerable attention in the recent literature, and it has been found that Pt–Pd bimetallic catalysts can exhibit unique properties, such as enhanced catalytic activity and better thermal stability, that either Pt-only or Pd-only catalyst do not possess. For example, alloying between Pt and Pd has been shown to lead to synergistic enhancement of propylene oxidation activity [9], and the addition of Pd to Pt catalysts tends to retard the sintering rate of Pt [10,11]. Furthermore, a relatively small amount of Pt added to Pd catalysts can suppress the particle growth and reduce the extent of water-induced Pd catalyst deactivation during methane oxidation [12,13].

With this background in mind, this study was undertaken to investigate the oxidation activity of aged Pt-only, Pd-only and Pt–Pd bimetallic catalysts for three different types of HCs. In this work, propylene was chosen as a representative light olefin, with propane and iso-pentane taken as surrogate HCs for n-alkanes and alkane isomers, respectively. The feedstream used for catalytic activity testing includes not only HC of specific interest and O₂, but also CO, H₂, NO and H₂O to simulate the actual exhaust environment [14]. It has been reported that HC oxidation over Pt and Pd is significantly affected by the presence of CO [15], H₂ [16], NO [17] and H₂O [18]. Moreover, the catalytic activity of Pd based catalyst is largely dependent on the oxygen concentration which determines the formation of PdO [19]. Although the phase of Pt is less sensitive to oxidative condition, the presence of Pt can change redox property of Pd [20,21]. Therefore, for our experiments, the O₂ concentration in the feed was varied to cover both near-stoichiometric and strongly oxidizing conditions to examine HC oxidation activities of the Pt/Pd catalysts with different Pt:Pd ratios under conditions likely to be encountered during the operation of conventional (stoichiometric) gasoline engines and lean-burn gasoline/diesel engines, respectively.

2. Experimental

2.1. Catalyst preparation and characterization

Three commercial Pt–Pd/Al₂O₃ catalysts with different Pt:Pd ratios, all washcoated on a ceramic monolith substrate (400 cells/in² with 4 mil wall thickness), were provided from GM Global R&D. The catalysts had Pt:Pd weight ratios of 50:0, 32:18 and 0:50 with a total noble metal loading of 50 g/ft³, corresponding to Pt:Pd atomic ratios of 1:0, 1:1, and 0:1, respectively. The catalysts were aged in a flow reactor at 900 °C for 100 h under lean-rich cycled feedstream conditions. The aging involved repeated exposure of the catalysts to a 3-minute duty cycle, which includes a 5-second pulse of 3% O₂ and a 5-second pulse of 3% CO, each injected into the background gas containing 10% H₂O, 10% CO₂ and N₂. Upon completion of the aging, the catalyst sample was cooled to room temperature in flowing N₂ to minimize the possibility of oxidation state changes during the cool down. Such a lean-rich cycling aging protocol was previously adopted to simulate the deactivation of commercial automotive catalysts during vehicle use [22,23]. The aged monolith catalysts were gently crushed and sieved to the size range of

650–850 μm for oxidation activity measurements and some characterization studies.

The Pd and Pd loadings of each sample were measured by inductively coupled plasma atomic emission spectroscopy (ICP-AES). The sieved catalysts in the range of 650–850 μm were pretreated in aqua regia, which is a 3:1 volumetric mixture of HCl and HNO₃ at 95 °C for 3 h. Then, the solution was analyzed by using Shimadzu model ICPS-8100.

The crystalline structures of the catalysts before and after the reactions were analyzed by X-ray diffraction (XRD) patterns taken from X-ray diffractometer (Rigaku) using a Cu Kα radiation source operated at 30 mA and 40 kV. The fine scan was performed to obtain patterns with high resolution in the region from 10 to 90°, with the scan speed and scanning step size of 1.0 °/min and 0.2°, respectively.

X-ray near edge absorption fine spectroscopy (XANES) in the range of Pd K-edge and Pt L3-edge was obtained at Pohang Accelerator Laboratory (7D-XAFS beamline in PLS-II). Si (111) crystal was adopted as monochromator with the ring current of 360 mA and the beam energy of 2.5 GeV. The energy scales were calibrated based on the well-known characteristics of Pd and Pt foils (24,350 eV and 11,564 eV, respectively). Ionization chamber for incident and transmitted beam were purged with 1 atm of N₂. The step and duration used for X-ray absorption near edge structure (XANES) analysis of Pd and Pt were 1 eV and 2 s, and 0.4 eV and 2 s, respectively. Athena software was utilized for energy calibration, background subtraction and normalization of the calibrated energy.

Scanning transmission electron microscopy (STEM) and energy dispersive spectroscopy (EDS) analysis were performed by JEM-2100 F transmission electron microscope (TEM, JEOL, Japan) equipped with field emission gun at accelerating voltage of 200 kV. Prior to the analysis, samples were finely ground, ultrasonically dispersed in absolute ethanol, suspended on holey carbon TEM grid, and then dried in an oven at 60 °C overnight. The average particle sizes of the catalysts were calculated by measuring more than 50 particles in STEM images. EDS mapping analysis was performed for the Pt–Pd bimetallic catalysts to determine the distributions of Pd and Pt in each particle. Meanwhile, the low magnified images of the catalysts were captured by field emission scanning electron microscopy (FE-SEM) in back scattered electron mode (MERLIN Compact, ZEISS).

Dispersions of Pd, Pt–Pd and Pt in the catalysts were measured by CO chemisorption conducted by BEL-CAT-II (BEL Japan Inc.). About 0.2 g of the sample was exposed under 5 vol.% H₂/Ar gas for 1 h at the temperature of 300 °C, where Pt, Pd and Pt–Pd were fully reduced. Then, the CO chemisorption was performed at 30 °C. The stoichiometric ratio of adsorbed CO to active metal at the surface atom was considered to be 1:1, not only for the monometallic catalyst but also for the Pt–Pd bimetallic catalyst, as reported [24]. The average particle size of active metal was also calculated from the dispersion.

Temperature programmed hydrogen reduction (H₂-TPR) profiles were obtained by BEL-CAT-II (BEL Japan Inc.). About 0.2 g of the sample was pretreated under 21 vol.% O₂/N₂ at 500 °C for 2 h, and cooled down to –90 °C. Then, TCD signal was collected during raising the temperature from –90 °C to 800 °C with the ramping rate of 10 °C/min while flowing the 5 vol.% H₂/Ar gas to the sample.

2.2. Catalytic reaction system and activity testing

All catalytic reactions were carried out using a 1/2 inch quartz tubular reactor housed inside a vertically mounted electric furnace. The sieved catalyst powder samples (0.1228 g; 650–850 μm in size) were loaded in the quartz reactor together with inert alumina beads (0.9500 g) so as to help dissipate the heat generated during the reaction.

One thermocouple, which controlled the furnace temperature, was located at the radial center of the quartz reactor and far from the catalytic bed to minimize the impact of the reaction exotherm. It was

confirmed that under inert N₂ flow, there was no significant temperature difference in the radial direction radial direction, with only slight axial temperature gradients (less than 2 °C) observed (Fig. S1 and Table S1). The catalyst temperatures at three different axial locations under reaction conditions were measured with the thermocouples whose tips were located in the top, middle and bottom of the catalytic bed. The axial temperature gradients inside the catalyst bed during the reaction were found to be within a few degrees even when the HC and CO conversions were near 100% (Fig. S2 and Table S2).

The feedstream used for activity testing consisted of hydrocarbon (HC), carbon monoxide (CO), hydrogen (H₂), nitric oxide (NO), oxygen (O₂) and water (H₂O), balanced with nitrogen (N₂). Only the concentration of O₂ was changed while keeping the concentrations of all other species constant in order to vary the stoichiometric factor (S), which is defined as $S = (2[O_2] + [NO])/([CO] + [H_2] + (3n + 1)[C_nH_{2n+2}] + 3n[C_nH_{2n}])$ [25–27]. The reactant gases were introduced through a 1/8 in. stainless steel tube, which was heated at 160 °C to prevent water condensation. The flow rates of all gases except water were controlled by mass flow controllers (MKS), while water was injected by a syringe pump. Total gas flow rate was maintained at 225 ccm, yielding a space velocity of 100,000 h⁻¹. It has been shown that there are no significant effects of external and internal mass transfer limitations under these experimental conditions [25].

In this study, we examined three different conditions for catalytic activity testing: slightly rich ($S = 0.96$), slightly lean ($S = 1.15$) and fully lean ($S = 11.3$) conditions. Prior to each test, all catalysts were pre-treated at 550 °C for 2 h in a gas stream containing 0.9% CO, 0.3% H₂, 10% H₂O and O₂ whose concentration level was chosen to provide the initial catalyst oxidation state similar to that expected to reach under the reaction condition of interest. The feedstream compositions used for pre-treatment and catalytic activity testing are presented in Table 1.

Three hydrocarbon species, propane (C₃H₈), propylene (C₃H₆) and iso-pentane (iso-C₅H₁₂) were chosen for the study of hydrocarbon oxidation activity. While propane and propylene are surrogates for light n-alkanes (straight-chain saturated HCs) and alkenes (unsaturated HCs), respectively, iso-pentane is a heavier saturated hydrocarbon with a branched structure (alkane isomer) which is present in significant quantities in engine exhaust [4,5].

The catalytic reactions were carried out as steady-state experiments. The furnace temperatures were raised typically from 250 °C to 500 °C at 50 °C intervals for the oxidations of saturated hydrocarbons, and from 180 °C to 360 °C at 30 °C intervals for the oxidation of propylene. In case of propylene oxidation over Pt/Al₂O₃ under near-stoichiometric condition, the temperature was raised from 240 °C to 450 °C. At each temperature point, the catalytic reaction was stabilized until the concentrations of all reactants and products were maintained, where the concentration data was obtained. The ramping rate between each temperature point was 2.5 °C/min to avoid overshooting of the target temperature. The reactions under the same condition were performed

repeatedly 2 or 3 times to obtain the reproduced result.

The reactant gases were analyzed simultaneously using an on-line gas chromatograph (Agilent 6890N) equipped with both thermal conductivity detector (TCD) and flame ionization detector (FID) as well as an on-line FT-IR spectrometer (Nicolet iS50, Thermo Scientific) with a 3 m gas cell. Both H₂ and O₂ were quantified by GC-TCD, while hydrocarbons, CO and CO₂ were analyzed by GC-FID. FT-IR was also used to measure the concentrations of hydrocarbons, CO, CO₂, NO, NH₃ and N₂O. All conversion data reported here was measured after reaching a steady state.

3. Results and discussion

3.1. Catalyst characterization after lean-rich cycling aging

The aged Pd-only, Pt-only and Pt–Pd monolith catalysts were gently crushed and sieved for reaction and characterization studies. Based on ICP-AES, the PGM loadings in Pd/Al₂O₃, Pt–Pd/Al₂O₃ and Pt/Al₂O₃ were all about 0.38 wt.%. In detail, 0.375 wt.% Pd for Pd/Al₂O₃; 0.136 wt.% Pd and 0.245 wt.% Pt for Pt–Pd/Al₂O₃; 0.380 wt.% Pt for Pt/Al₂O₃. The XRD patterns of the catalyst samples are dominated by highly crystalline peaks arising from the cordierite substrate (Fig. S3). However, zoomed-in XRD patterns between 2θ values of 39 and 41° (see Fig. 1(a)) clearly show the metallic Pt(111) and Pd(111) peaks for the monometallic Pt and Pd catalysts, respectively. In case of the bimetallic Pt–Pd/Al₂O₃ catalyst, a peak was located between the Pt(111) and Pd(111) peaks, indicating the formation of Pt–Pd alloy phase [28]. The presence of Pt and Pd oxide peaks, however, was difficult to be detected due to overlap with the cordierite peaks in the XRD patterns. Thus, the oxidation states of the catalysts were analyzed by XANES and the results are shown in Fig. 1(b) and (c). The Pd K-edge and Pt L3-edge XANES spectra of the aged monometallic and bimetallic catalysts were almost identical to those of Pd and Pt foils, respectively, which demonstrates that the bulk of Pd and Pt particles in all three aged catalysts existed as their metallic phases. This is reasonable because metallic phases are thermodynamically favored at the high temperature (900 °C) used for the catalyst aging [29], and the metallic phase would have been maintained during cooling to room temperature in N₂ after aging.

We further characterized the individual metal particles by using STEM and EDS mapping. As shown in Fig. 2(a), the metal particles of the Pt–Pd catalyst mainly existed as large faceted particles on the aggregated alumina particles in line with the XRD pattern. The Pt and Pd distributions in the bimetallic particles of the Pt–Pd/Al₂O₃ catalyst were investigated by STEM with EDS. The EDS mapping measurement demonstrates that homogeneous Pt–Pd alloys were formed after the lean-rich cycling aging (Fig. 2(b)), although the composition of each particle showed some deviation from its average value. The aged catalysts exhibited broad size distributions with average metal particle sizes (and their standard deviations) for the Pd, Pt–Pd and Pt catalysts of 63 (± 20), 35 (± 13) and 40 (± 24 nm), respectively (Fig. 2(c)).

Table 1
Compositions of pre-treatment and reaction gases depending on reaction conditions.

	Slightly rich condition		Slightly lean condition		Fully lean condition	
	Pre-treatment	Reaction	Pre-treatment	Reaction	Pre-treatment	Reaction
HCs (ppm C1 base) (ppm)	–	1500	–	1500	–	1500
CO (%)	0.9	1	0.9	1	0.9	1
H ₂ (%)	0.3	0.3	0.3	0.3	0.3	0.3
NO (ppm)	–	500	–	500	–	500
O ₂ (%)	0.55	0.83	0.75	1	10	10
H ₂ O (%)	10	10	10	10	10	10
Stoichiometric factor (S)	0.92	0.95 (C ₃ H ₈)	1.25	1.14 (C ₃ H ₈)	16.7	11.1 (C ₃ H ₈)
		0.96 (iso-C ₅ H ₁₂)		1.15 (iso-C ₅ H ₁₂)		11.3 (iso-C ₅ H ₁₂)
		0.98 (C ₃ H ₆)		1.17 (C ₃ H ₆)		11.5 (C ₃ H ₆)
Space velocity	100,000 h ⁻¹					

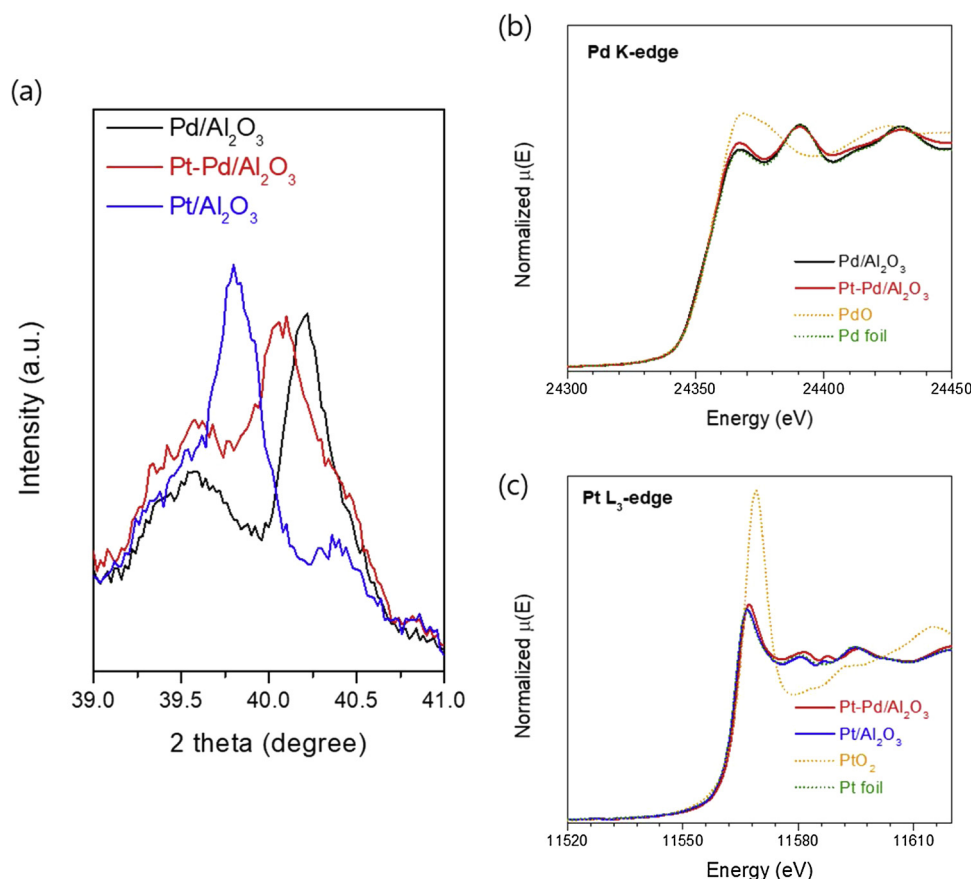


Fig. 1. The zoomed-in XRD patterns around the characteristic peaks of metallic Pt and Pd of aged Pt-only, Pd-only and Pt–Pd catalysts (a); normalized XANES for Pd K-edge (b) and Pt L3-edge (c) of aged monometallic and bimetallic catalysts.

The size distributions of metal particles after lean/rich cycling aging were observed to be quite broad (Fig. S4). The Pt–Pd/Al₂O₃ catalyst had the smallest average particle size, indicating that the particle growth by Ostwald ripening sintering was retarded due to the formation of a Pt–Pd alloy phase [10,30]. The dispersion of the metal in the catalyst was also obtained from CO chemisorption analysis, and the average particle sizes were calculated from the dispersion as reported in elsewhere [22,24]. The dispersions (the average particle sizes) of Pd, Pt–Pd and Pt were 1.56% (72 nm), 2.79% (41 nm) and 1.93% (59 nm), respectively. The values of the average particle sizes were a little different from those from STEM images, but the order of average size was identical in both cases of STEM and CO chemisorption, which was Pd/Al₂O₃ > Pt/Al₂O₃ > Pt–Pd/Al₂O₃.

It is rather surprising that the average metal particle size of the monometallic Pt catalyst was smaller than that of the monometallic Pd catalyst in view of the literature reports that Pt particles are severely sintered after hydrothermal aging under lean conditions [11,31]. However, we did not observe considerably large particles by FE-SEM with back-scattered electron mode (Fig. S5). Thus, our results suggest that the exposure of the Pt catalyst to the lean-rich cycling atmosphere during aging led to much less severe particle growth than expected when aging in a continuously lean atmosphere. It is possible that the formation of volatile PtO₂ species may be suppressed under the lean-rich cycling condition. Furthermore, Pd sintering behavior under lean-rich cycling conditions is not well understood, although Pd is known to be more susceptible to sintering under rich conditions than under lean conditions [32]. Note also that the number of noble metal atoms in the Pt/Al₂O₃ catalyst was almost half that in the Pd/Al₂O₃ catalyst, which could also affect the sintering rate of the metal particles.

Fig. 3 displays the H₂-TPR profiles of Pd/Al₂O₃, Pt–Pd/Al₂O₃ and Pt/Al₂O₃ catalysts. Since all samples were initially the metallic phases

(Fig. 1), the H₂ consumption in Fig. 3 originated from the reduction of the oxidized species formed during the pretreatment under 21% O₂/N₂ at 500 °C for 2 h. The H₂ consumption over Pt/Al₂O₃ catalyst was barely observed in the entire temperature range. In our previous study, while small-sized Pt/Al₂O₃ exhibited several peaks arising from Pt species weakly and strongly interacting with Al₂O₃, such peaks disappeared with Pt aggregation [33]. Thus, the absence of peak in Pt/Al₂O₃ is attributed to its large Pt cluster size (~40 nm). In contrast, Pd/Al₂O₃ had two positive peaks and one negative peak. The two positive peaks at around 0 °C and 30 °C are generally designated as reduction of PdO and formation of PdH_x, respectively, while the negative peak at around 60 °C originates from the decomposition of PdH_x [34,35]. It indicates that the formation of PdO occurred thermodynamically easily in spite of the large Pd size in Pd/Al₂O₃ compared to that of Pt in Pt/Al₂O₃. Meanwhile, the consumed H₂ amount of Pt–Pd/Al₂O₃ was one-third of that of Pd/Al₂O₃, in line with the amount of Pd content. In addition, note that no oxidized species existed in Pt/Al₂O₃. Thus, the peak of Pt–Pd/Al₂O₃ is thought to originate from the oxidized Pd species. The peak position of Pt–Pd/Al₂O₃ located at around –20 °C, which was quite lower temperature compared to the peaks from Pd/Al₂O₃. Comparing Pt–Pd/Al₂O₃ to Pd/Al₂O₃, the shift of peak position to the lower temperature indicates that the facile reduction of Pd oxide in Pt–Pd/Al₂O₃ was promoted by the presence of Pt.

3.2. Hydrocarbon oxidation under near-stoichiometry conditions

The oxidation reactions of propane, iso-pentane and propylene were carried out over the aged Pt, Pd and Pt–Pd catalysts under the slightly lean condition (*S* = 1.15). Recall that in addition to HC and O₂, the feedstream also included CO, H₂, NO and H₂O to simulate gasoline engine exhaust conditions (see Table 1 for feedstream composition). In

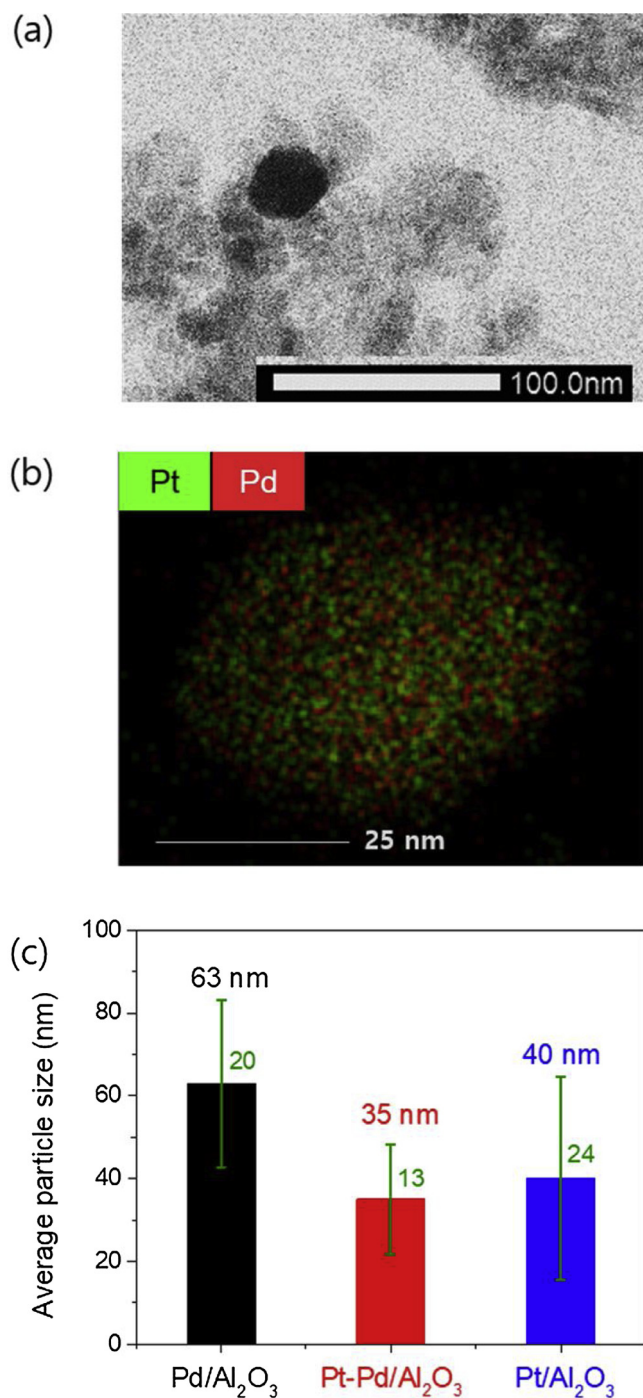


Fig. 2. The representative STEM image of aged Pt-Pd/Al₂O₃ catalyst (a); the distributions of Pt and Pd in a bimetallic particle of aged Pt-Pd/Al₂O₃ catalyst analyzed by EDS mapping (b); average particle sizes of aged Pt-only, Pd-only and Pt-Pd catalysts with their standard deviations (c).

case of propane oxidation, the Pt/Al₂O₃ catalyst showed the best performance followed by the Pd/Al₂O₃ and Pt-Pd/Al₂O₃ catalysts, with the propane conversions over Pt, Pd and Pt-Pd catalysts at 400 °C being ~88%, ~34% and ~16%, respectively (see Fig. 4(a)). The observation of a steep rise in propane conversion (Fig. 4(a)) and CO conversion (Fig. S6(b)) light-off over Pt/Al₂O₃ in the same temperature range (300–350 °C) is likely to be related to the strong adsorption of CO on the Pt surface. This causes the blocking of the active sites (leading to suppression of the reactions by “CO poisoning”) until a sufficiently high temperature is reached to start to desorb CO from the surface

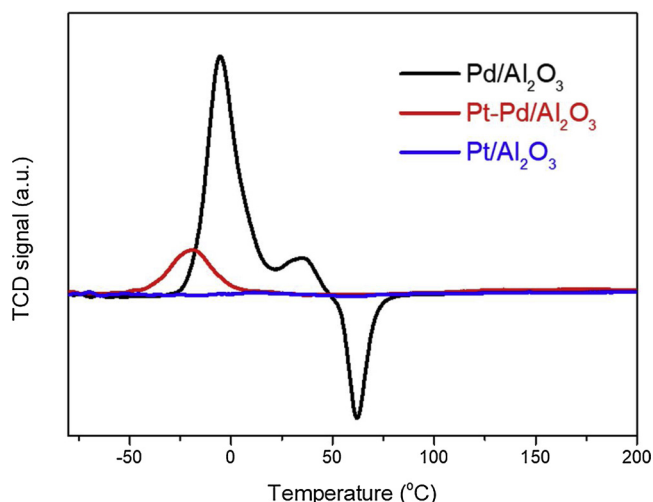


Fig. 3. The temperature programmed hydrogen reduction (H₂-TPR) profiles of Pd/Al₂O₃, Pt-Pd/Al₂O₃ and Pt/Al₂O₃ catalysts.

[24,36,37]. Interestingly, the activity of Pt-Pd/Al₂O₃ was significantly lower than that of either Pd/Al₂O₃ or Pt/Al₂O₃, indicating that the formation of Pt-Pd alloy is detrimental for the propane oxidation at S = ~1.15.

As shown in Fig. 4(b), the Pt/Al₂O₃ catalyst was also the most active for the iso-pentane oxidation; however, unlike for propane oxidation, Pt-Pd/Al₂O₃ was observed to be more active than Pd/Al₂O₃. There were similarities in the CO and NO conversion behavior as well as the byproduct (NH₃ and N₂O) formation between the cases of propane oxidation (Fig. S6) and iso-pentane oxidation (Fig. S7). For example, the CO conversions during both propane and iso-pentane oxidations were the highest over Pd/Al₂O₃ followed by Pt-Pd/Al₂O₃ and Pt/Al₂O₃ (Figs. S6(b) and S7(b)). In addition, in both Figs. S6(c) and S7(c), the Pd-only catalyst showed higher NO conversion than the Pt-only catalyst at low temperatures (250–350 °C), while the trend was reversed at higher temperatures. Furthermore, in both cases, the major product from NO reduction at low temperature (~260 °C) over the bimetallic Pt-Pd catalyst was NH₃, whereas N₂O was mainly formed over the Pd-only catalyst during the NO reduction reaction. These similarities in the CO/NO conversion vs. temperature data shown in Figs. S6 and S7 can be explained by the fact that these saturated hydrocarbons (i.e., propane and iso-pentane) do not adsorb well on the metal surface [38], and thus their types or presence in the feedstream do not significantly affect the CO oxidation and NO reduction reactions.

Concerning the order of the hydrocarbon oxidation activity of Pt-only and Pd-only catalysts, Pt catalyst is known to be more active for the oxidation of heavy saturated hydrocarbon than Pd catalyst under simple feed condition, although Pd catalyst has higher activity for methane oxidation [6,15,39,40]. Our result also proved that Pt-only catalyst has higher activity for the oxidation of the C3 and C5 saturated hydrocarbons than Pd-only catalyst even under the practical exhaust gas condition including CO, H₂, NO and H₂O (see Fig. 4(a) and (b)). Meanwhile, the Pt-Pd alloy catalyst is the mixture of Pt and Pd metals, but it did not have any trend of the catalytic activity compared to the monometallic catalysts. Specifically, while the activity of propane oxidation was lower than over the monometallic catalysts, the activity order of iso-pentane oxidation over the Pt-Pd alloy catalyst was located between the monometallic catalysts. Similarly, Epling et al. observed that the activity order of Pt-Pd bimetallic catalysts with different Pt/Pd ratios was varied by the species of hydrocarbon without any trend [24]. Such different oxidation behavior of hydrocarbons might be related to the changes in the characteristic properties of Pt-Pd alloy from those of the monometallic catalysts as identified in Section 3.1. However, unfortunately, we could not concretely identify how the changes in the

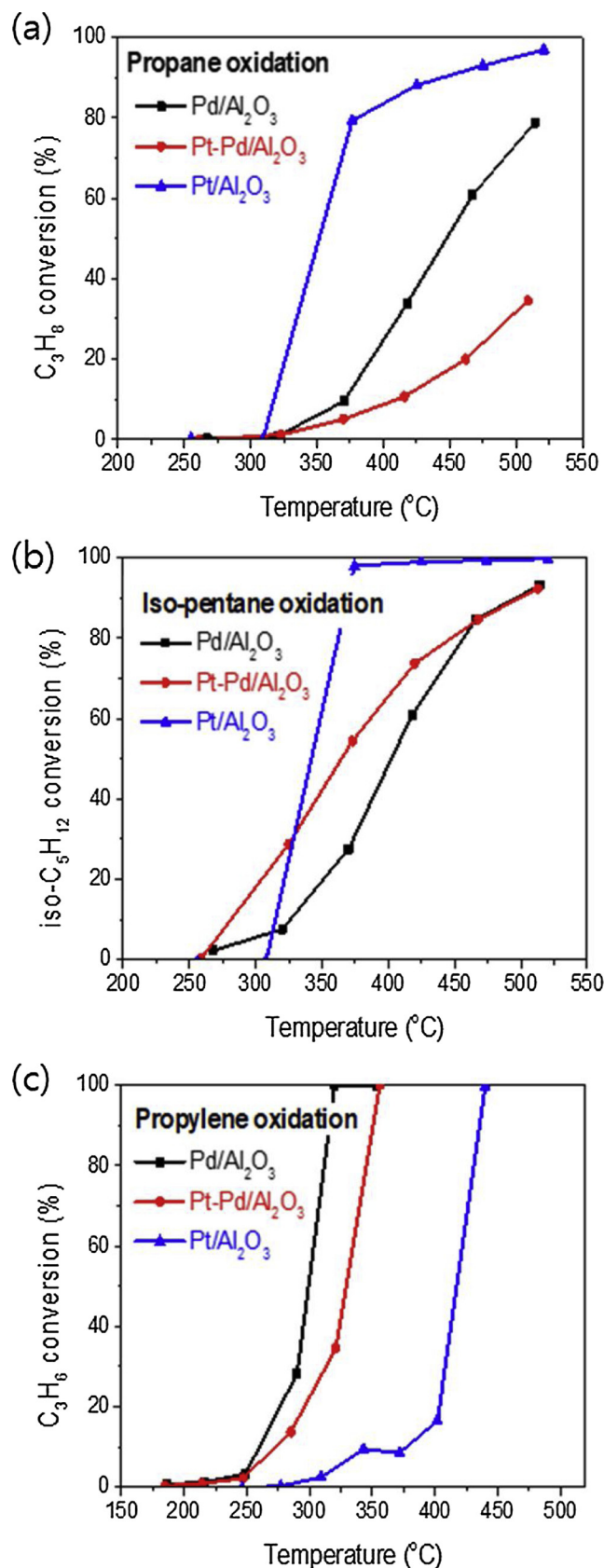


Fig. 4. The conversions of propane (a), iso-pentane (b) and propylene (c) over Pd-only, Pt-only and Pt-Pd catalysts under slightly lean condition ($S = \sim 1.15$).

characteristic properties of Pt-Pd alloy affect the oxidations of hydrocarbon, since hydrocarbon oxidation is related to various unpredictable factors such as the energies of C–H or C–C bond cleavage, reaction mechanisms, and competitive adsorption of reactants.

In contrast to the saturated hydrocarbons, unsaturated hydrocarbons tend to adsorb on the noble metal catalyst surface rather strongly [41], and their oxidation behavior in the presence of CO is closely coupled with the CO oxidation due to the competitive adsorption of CO and HC on the metal surface [7,15,18,42]. As shown in Fig. 4(c), complete conversion of propylene was achieved over the Pd, Pt-Pd, and Pt catalysts at 319, 355 and 440 °C, respectively, indicating that the propylene oxidation activity decreases in the order of Pd > Pt-Pd > Pt. Although the oxidation of CO generally started at a somewhat lower temperature than that of C₃H₆, both CO and C₃H₆ reached 100% conversion at approximately the same temperature over all the catalysts. Interestingly, in the presence of CO in the feedstream, the 50% conversion temperature for propylene oxidation over the Pt/Al₂O₃ catalyst was much higher than that for the propane oxidation. This is a rather surprising observation as propylene itself is known to be more reactive than propane [6,7]. Such phenomenon can be explained based on the competition of the co-adsorbed CO and propylene for a limited amount of adsorbed oxygen on the catalyst surface under reaction conditions, in other words, the CO poisoning. The order of propylene oxidation activity can also be rationalized by the CO poisoning, because the CO oxidation is generally more active over Pd-only catalyst than over Pt-only catalyst [7,24,43]. In addition, the NO conversion vs. temperature behavior observed during propylene oxidation was also quite different from that during the oxidation of saturated hydrocarbons (compare Figs. S6(c), S7(c) and S8(c)). This is because, unlike saturated hydrocarbon, propylene actively competes with NO to adsorb on the catalyst surface. The NO conversion over all the catalysts during propylene oxidation appears to increase gradually and monotonically with increasing temperature, reaching a maximum conversion of only ~30%.

As observed in Fig. 4, the oxidation reactions over Pt/Al₂O₃ are initiated at ~250–300 °C where CO starts to desorb from the surface, thereby creating vacant sites for oxygen adsorption. The CO conversion increases more rapidly than propylene conversion in the temperature range of 250–340 °C probably because CO is more reactive than propylene toward surface oxygen at low temperatures [18,44] and the activation of propylene oxidation, unlike CO oxidation, likely requires multiple adjacent sites for dissociative adsorption of propylene [7]. In addition, Wang et al. reported the oxidation of propylene might start at the metal site whose surface is partially reduced by CO ignition [45]. Between 340 and 400 °C, the CO conversion drops while the propylene conversion gradually increases. This can be attributed to the fact that the rate of propylene oxidation becomes higher than CO oxidation at these higher temperatures due to its higher activation energy [44] and/or stronger dependence on O₂ concentration [7], so that the propylene conversion increases at the expense of decreasing CO conversion in this temperature regime, as observed in Figs. 4(c) and S8(b).

The oxidation states of Pt and Pd metals after the reactions (i.e., oxidation of propane followed by iso-pentane and then propylene) under the slightly lean condition were analyzed by XANES, with the results shown in Fig. 5(a) and (b). It can be seen that there was very little change in the Pd K-edge and Pt L3-edge spectra from the spectra taken before reaction (shown in Fig. 1(b) and 1(c)), demonstrating that the oxidation states of the noble metals in the catalysts did not change after several reactions under the slightly lean condition. This observation is consistent with the literature reports that oxygen is chemisorbed on the surface of Pd particles at low oxygen pressures, with no bulk oxidation occurring until the oxygen pressure becomes sufficiently high [19,46]. In addition, it was shown that the metallic phase is favored for large Pd particles [47]. Considering the large Pd particle size (~63 nm) as well as the low oxygen pressure (~1 kPa) and the co-presence of reductants in the feed, the bulk state of Pd is expected to remain as the

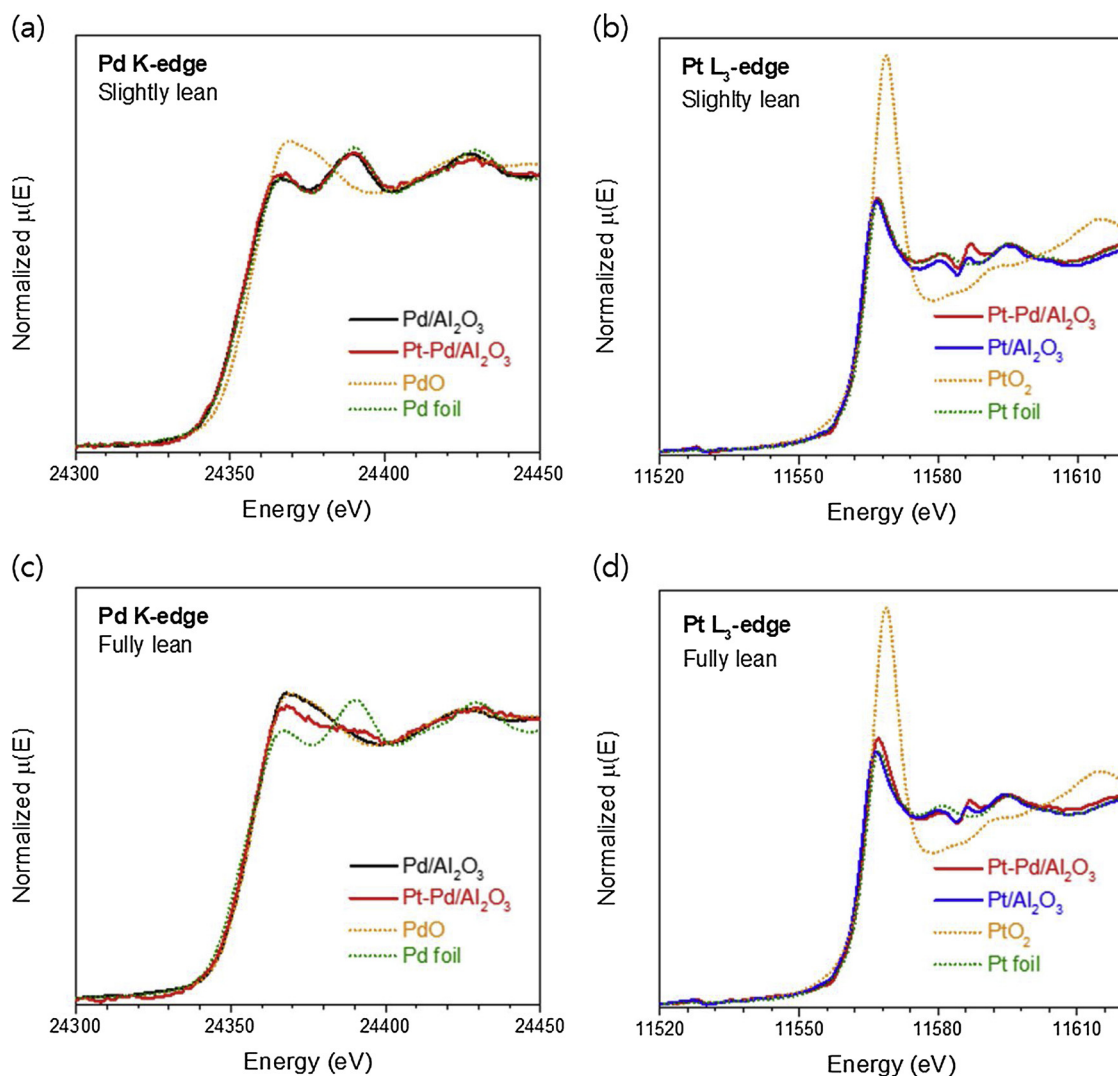


Fig. 5. The normalized Pd K-edge XANES of Pd-only and Pt-Pd catalysts after the reactions under slightly lean ($S = \sim 1.15$) (a) and fully lean ($S = \sim 11.3$) (c) conditions, and normalized Pt L₃-edge of Pt- only and Pt-Pd catalysts after the reactions under slightly lean ($S = \sim 1.15$) (b) and fully lean ($S = \sim 11.3$) (d) conditions.

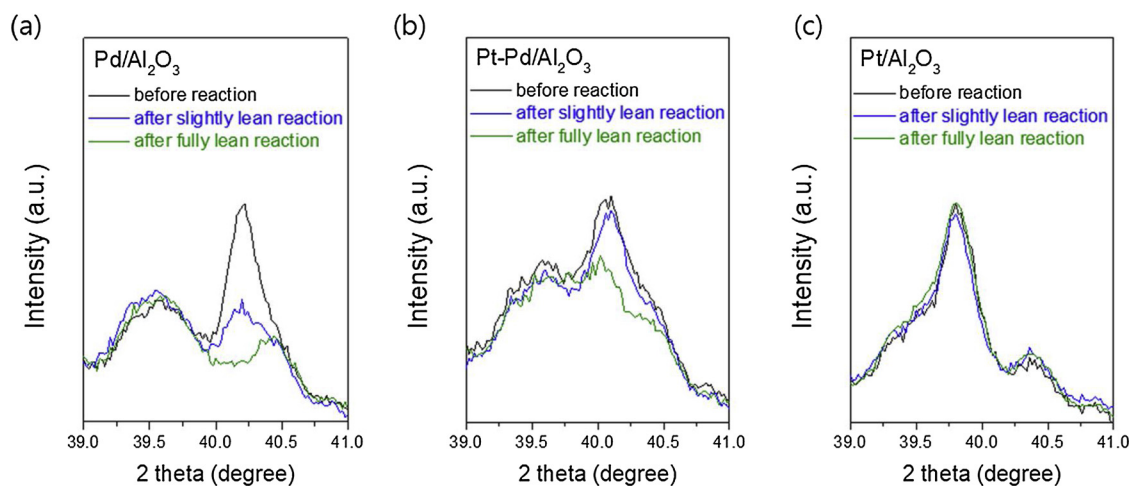


Fig. 6. The XRD patterns of Pd/Al₂O₃ (a), Pt-Pd/Al₂O₃ (b) and Pt/Al₂O₃ (c) catalysts before and after the reactions under slightly lean ($S = \sim 1.15$) and fully lean ($S = \sim 11.3$) conditions.

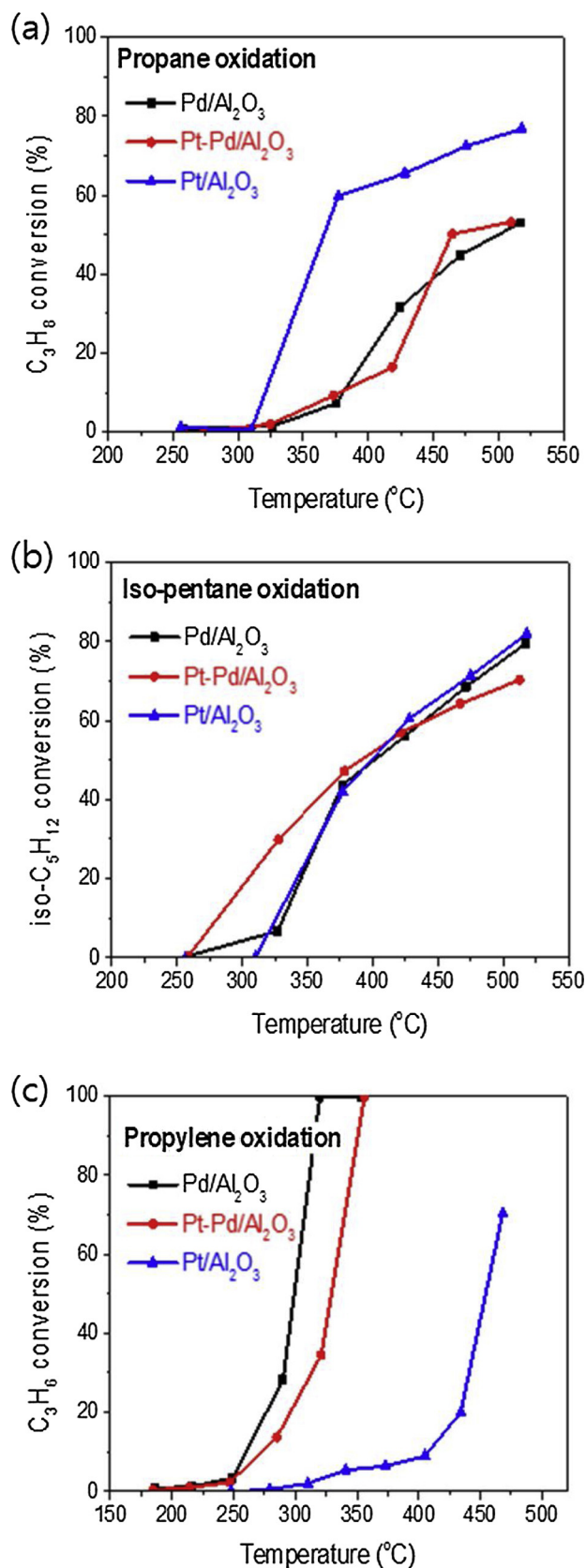


Fig. 7. The conversions of propane (a), iso-pentane (b) and propylene (c) over Pd-only, Pt-only and Pt-Pd catalysts under slightly rich condition ($S \approx 0.96$).

metallic phase during and after the reactions. Since the bulk oxidation of Pt is more difficult than that of Pd, the Pt metal particles in the Pt/Al₂O₃ and Pt-Pd/Al₂O₃ catalysts would also be in the metallic phase.

Fig. 6 shows the XRD patterns of the Pd, Pt-Pd and Pt catalysts after several reactions under the slightly lean condition. Compared to the initial state of the Pd catalysts (i.e., before reaction), the intensity of the Pd(111) peak decreased significantly after the reactions without changing its position. Since bulk Pd was not oxidized after the reactions as evidenced by the XANES results, this decrease in the XRD peak intensity was likely caused by a change in the crystalline structure of Pd. The XRD patterns for the Pt and Pt-Pd bimetallic catalysts, however, showed little change in the metallic peaks after reaction, indicating the higher stability of the crystalline metal particles. This observation is consistent with the fact that Pt is a metal which is not readily oxidized, and that Pt can promote the reducibility of PdO and/or stabilize the metallic state of the Pd [48]. In summary, the XANES and XRD results discussed above strongly suggest that the oxidation reactions under the slightly lean condition considered here take place on the metallic Pd surface partially covered with chemisorbed oxygen.

The conversion data obtained during the oxidation of the three hydrocarbons under the slightly rich condition ($S \approx 0.96$) listed in Table 1 are summarized in Fig. 7. The essential features of the hydrocarbon oxidation behavior in the low conversion regime (including the temperatures required for the onset of the oxidation reaction for each of the hydrocarbons) were nearly identical to those observed under the slightly lean condition ($S \approx 1.15$) discussed above. It is because, as the oxidations of HCs or CO barely occurred at such low temperature, only slight difference in the partial pressure of O₂ (i.e. 0.83 vol.% vs. 1.0 vol.%) would affect the oxidation activity under between slightly lean and rich condition. However, in high temperature region, where CO oxidation was completed, the O₂ concentration decreased sufficiently enough to decrease the chemisorbed oxygen, which leads to the adsorptions of other species such as NO and CO on metal surface. This would cause totally different oxidation behavior of hydrocarbon and reduction behavior of NO between under slightly lean and slightly rich conditions in high temperature region with low oxygen concentration. Thus, the high-temperature oxidation activities for the saturated hydrocarbons at $S \approx 0.96$ were adversely affected by the lower O₂ concentration in the slightly rich feed, providing lower maximum hydrocarbon conversion levels than those attained at $S \approx 1.15$. In addition, the conversion of propylene over Pt/Al₂O₃ in the high temperature region (> 400 °C) were significantly lower than that observed under the slightly lean condition shown in Fig. 4(c). More specifically, the propane conversion over the Pt-Pd/Al₂O₃ catalyst in Fig. 7(a) increased sharply between 400 and 450 °C, which was not observed under the slightly lean conditions. The conversion of iso-pentane over Pt/Al₂O₃ in the high temperature region was significantly lower than that observed under slightly lean condition shown in Fig. 4(b). There were also some decreases in H₂ and CO conversions at high temperature possibly originating from the partial oxidation or the steam reforming of hydrocarbons (Figs. S9 and S10). On the other hand, the results of NO conversions showed greatly different trend compared with the result from slightly lean reactions. During the propane oxidation test, the NO conversion was started to increase again at 370–420 °C, where NO acts as oxidant, which can be attributed to the deficient O₂ concentration (Fig. S9). The NO conversion trend is quite different during iso-pentane and propylene oxidation, but NO conversion also increased at high temperature (Figs. S10 and S11), which can also be attributed to the effect of chemisorbed oxygen atoms on metal surface.

3.3. Hydrocarbon oxidation under fully lean condition

As discussed above, Pt and Pd in all the catalysts used in this study existed as their metallic phases before and after reaction under the slightly lean condition ($S \approx 1.15$ with 1% O₂ in the feed). However, it is expected that the phases of Pt and Pd would eventually change as we

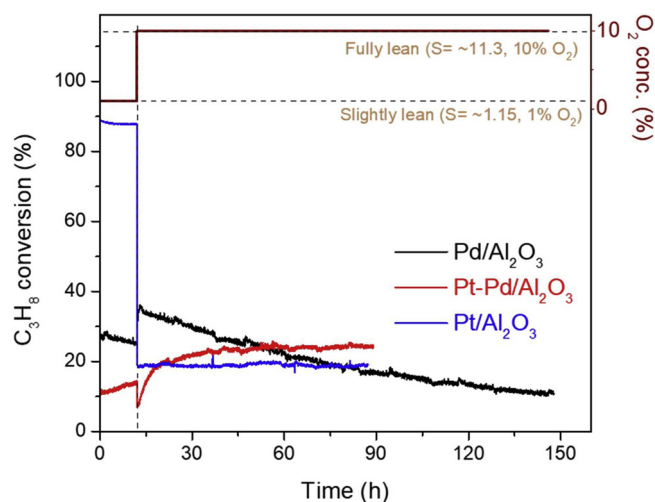


Fig. 8. The changes in propane conversion with time-on-stream after increasing the O_2 concentration from 1% to 10% at 400 °C.

move toward fully lean conditions ($S \approx 11.3$ with 10% O_2 in the feed) characteristic of lean-burn gasoline engine exhaust. To examine how the catalyst oxidation activities change in response to a gas stream containing a large excess of oxygen, the oxygen concentration was increased during the propane oxidation reaction. After running the propane oxidation under the slightly lean condition at 400 °C for 12 h, the oxygen concentration was increased abruptly from 1% to 10% (while keeping the concentrations of all other species unchanged) and the propane conversion was monitored as a function of time under the fully lean condition. The observed changes in propane conversion over the Pt, Pd and Pt–Pd catalysts with time-on-stream are shown in Fig. 8. Immediately following the oxygen concentration increased, the propane conversion over the monometallic Pd catalyst increased abruptly from 25% to 36%, and then continuously decreased with time-on-stream over a period of ~135 h. On the other hand, the propane conversion of the bimetallic Pt–Pd catalyst initially decreased from 12% to 6.8%, and then increased monotonically with time-on-stream, approaching 24% after the reaction in the fully lean gas stream for 78 h. In case of the monometallic Pt catalyst, the propane conversion decreased precipitously from 88 to 19% at the time of increasing O_2 concentration, followed by a rapid stabilization. The initial changes in the propane conversion shown in Fig. 8 reflect the effect of the gas composition change on the propane oxidation rate. According to the previous study by Yao, the reaction orders in O_2 concentration for propane oxidation over Pt/ Al_2O_3 and Pd/ Al_2O_3 are about -1 and 0.1 [6], respectively. Furthermore, similar results were observed by Fujitani et al. with -2.5 and 1.6 of O_2 reaction orders over Pt/ Al_2O_3 and Pd/ Al_2O_3 , respectively [49]. Thus, this explains the large decrease and slight increase in propane conversion observed in Fig. 8 over the Pt/ Al_2O_3 and Pd/ Al_2O_3

catalysts, respectively, when increasing the O_2 concentration from 1 to 10%.

The changes in propane conversion with time-on-stream discussed above can be rationalized based on the change of the catalyst state during the reaction. To examine possible changes in the oxidation states of Pt and Pd after the exposure to the fully lean condition, the catalysts were analyzed by XANES after the reactions (Fig. 5(c) and (d)). Pd metals in the Pd/ Al_2O_3 and Pt–Pd/ Al_2O_3 catalysts were completely and partially oxidized, respectively, after the long-time exposure to the fully lean feed, as shown by the Pd K-edge spectra in Fig. 5(c). Compared to complete oxidation of Pd in the Pd/ Al_2O_3 catalyst, the partial oxidation of Pd in the Pt–Pd/ Al_2O_3 catalyst is explained by the H_2 -TPR (Fig. 3) result that PdO can be more easily reduced in the presence of Pt. On the other hand, the Pt L3-edge spectra in Fig. 5(d) shows that Pt species in both the Pt/ Al_2O_3 and Pt–Pd/ Al_2O_3 catalysts remained as the metallic phase even after the reaction under the fully lean condition, also in good agreement with the H_2 -TPR result. The rapid stabilization of the propane conversion over the Pt/ Al_2O_3 catalyst after the O_2 concentration change in Fig. 8 can be attributed to the fact that the metallic phase of Pt remained unchanged throughout the duration of the transient experiment. On the other hand, the activity of Pd/ Al_2O_3 continued to decrease slowly over a period of ~135 h, which is believed to be related to the gradual oxidation of Pd metal to PdO. It is well known that the presence of H_2O in the gas phase generally accelerates metal sintering and support deactivation, and can also have a particularly detrimental effect on the activity of PdO due to the formation of inactive Pd(OH)₂ species [50,51]. Since the catalysts had been aged at 900 °C in a wet gaseous environment prior to the reaction, the possibility of additional catalyst activity deterioration during the reaction at 400 °C due to support deactivation and/or metal sintering can be ruled out. Thus, the oxidation of Pd and the consequent formation of Pd(OH)₂ may likely be the primary cause for the slow decline in propane conversion shown in Fig. 8. The Pt–Pd bimetallic catalyst, however, showed completely different behavior after increasing O_2 concentration. After the initial decrease in activity, the propane conversion continuously increased with time-on-stream, eventually reaching the highest conversion among the three catalysts.

To explore the nature and origin of the partially oxidized Pd species in Pt–Pd catalysts which was confirmed by XANES, we analyzed the metal particles in Pt–Pd/ Al_2O_3 using STEM equipped with EDS. The EDS mapping results show that while some particles maintain homogeneous distribution of Pt and Pd (Fig. 9(a)), others show significant segregation of Pt and Pd (Fig. 9(b) and (c)). It is reasonable to hypothesize that it is the Pd from the de-alloyed Pt–Pd particles that is partially oxidized. Similar “excess” PdO that exists as a separate phase has been reported to play an important role in decreasing the sintering rate of Pt–Pd bimetallic catalysts [52]. It is unclear, however, how de-alloying and the attendant partial oxidation of Pd led to the gradual increase in propane oxidation activity with time-on-stream, as observed in Fig. 8. We also note that the Pt–Pd/ Al_2O_3 catalyst was stabilized

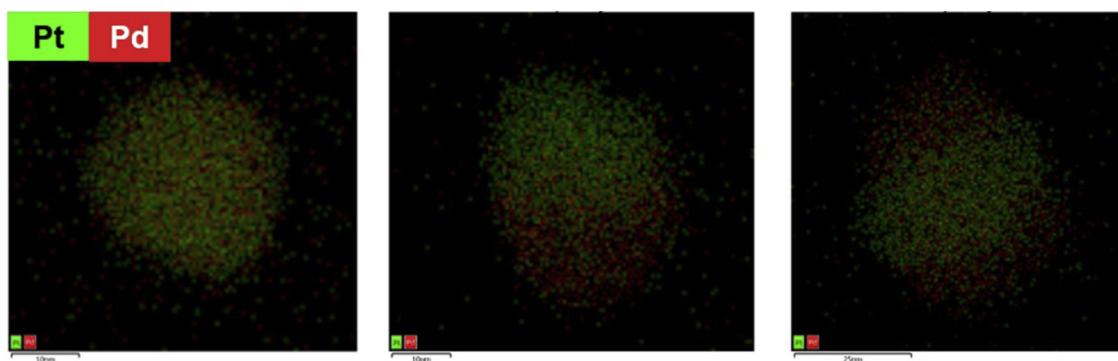


Fig. 9. The representative STEM-EDS image of Pt–Pd/ Al_2O_3 catalyst after the reactions under fully lean condition ($S \approx 11.3$).

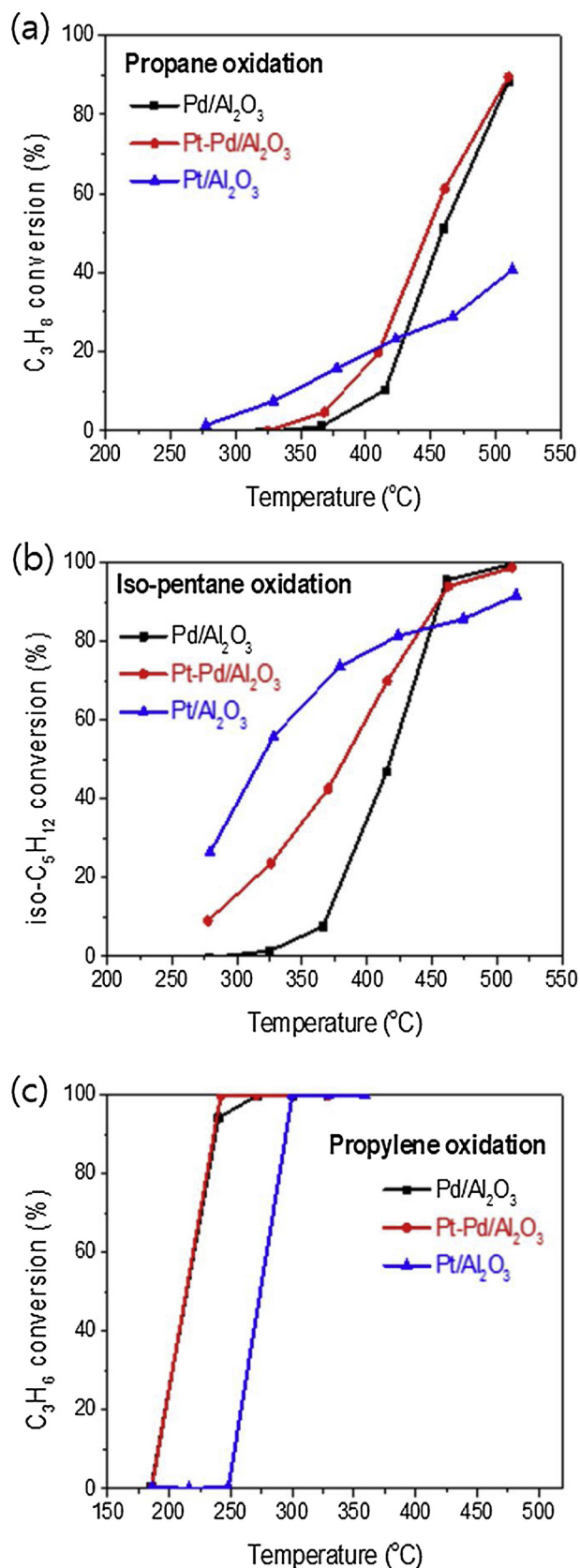


Fig. 10. The conversions propane (a), iso-pentane (b) and propylene (c) over Pd-only, Pt-only and Pt–Pd catalysts under fully lean condition ($S = \sim 11.3$).

more quickly than the Pd/Al₂O₃ catalyst after the change in oxygen concentration, which suggests that Pt plays a role in stabilizing Pd against the H₂O poisoning effect discussed above.

After the long-time stabilization of the catalysts at 400 °C during propane oxidation (as illustrated in Fig. 8), a series of light-off tests of hydrocarbon oxidation were carried out under the fully lean condition, with the results shown in Fig. 10. Overall, the activity order for the oxidation of saturated hydrocarbons was different from that observed under the near-stoichiometric conditions. In case of propane oxidation, the Pt/Al₂O₃ catalyst showed the highest activity at low temperature (< 400 °C) as observed under the near-stoichiometric conditions. It should be noted that the CO conversion under fully lean condition were already 100% at ~270 °C over all three catalysts (Figs. S12–S14). Because poisoning effect of CO on active site was largely eliminated at temperatures higher than 270 °C, the Pt/Al₂O₃ catalyst showed distinguishable activity of propane and iso-pentane oxidation at low temperature (270–400 °C) under fully lean condition. However, due to the sluggish increase with temperature in propane conversion over the Pt/Al₂O₃ catalyst originating from the low activation energy, the activity order in the high-temperature region (> 420 °C) under the fully lean condition changed to Pt–Pd/Al₂O₃ > Pd/Al₂O₃ > Pt/Al₂O₃. Similar changes in the reaction order was also observed in case of iso-pentane oxidation (Fig. 10(b)). Wise et al. and Renken et al. observed lower activation energy of propane oxidation over Pt catalyst than that over Pd [53,54]. Thus, such result indicates that the activation energies of not only propane oxidation but also iso-pentane oxidation are lower over Pt/Al₂O₃ than over Pd/Al₂O₃. On the other hand, the oxidation behavior over Pt–Pd/Al₂O₃ catalyst under fully lean condition seems to be located between those of Pt/Al₂O₃ and Pd/Al₂O₃, unlike the case under the stoichiometric condition in Section 3.2. The STEM-EDS images evidently showed that some Pt–Pd particles was de-alloyed after long-time exposure to the highly oxidative condition (Fig. 9). In addition, the presence of PdO in XANES spectra indirectly indicated that Pd metal was segregated from Pt–Pd alloy and then oxidized. As the Pt–Pd/Al₂O₃ catalyst after fully lean stabilization had both Pd-only surface and Pt-only surface, the intermediate activity of the Pt–Pd/Al₂O₃ catalyst in Fig. 10 can be explained.

When comparing the propane oxidation activity over the Pt/Al₂O₃ catalyst under stoichiometric and fully lean conditions, the high surface coverage by oxygen (whose adsorption strength is stronger than propane) in the presence of a large excess of oxygen seems to exclude the adsorption of propane on the Pt surface, resulting in the significantly reduced activity under fully lean condition. In case of iso-pentane oxidation, the high activity of the Pt/Al₂O₃ catalyst is mostly retained even under the fully lean condition (compare Figs. 4(b) vs 10 (b)), indicating that the iso-pentane oxidation was less affected by the adsorption of oxygen. This is possibly related to the adsorption ability of alkane on metal surface, as Weinberg et al. observed that the desorption temperature of adsorbed alkane was delayed with the longer chain length over Pt surface [55]. Iso-pentane might adsorb more easily on metal surface than propane, resulting in less sensitive to the oxygen concentration. The propylene oxidation activities of all three catalysts, on the other hand, were greatly enhanced under the fully lean condition compared to the slightly lean condition (compare Figs. 4(c) vs 10 (c)) because its oxidation rate is limited by the low oxygen coverage on the surface due to the much stronger adsorption of propylene and CO compared to oxygen. In the presence of a large excess of oxygen in the fully lean feed, the NO reduction reaction did not occur (thus there was no NH₃ and N₂O formation), but significant amounts of NO were oxidized to NO₂ over the Pt-containing catalysts (Pt/Al₂O₃ and Pt–Pd/Al₂O₃) at temperatures higher than 250 °C (Figs. S12–S14). As expected, the Pt-containing catalysts (Pt/Al₂O₃ and Pt–Pd/Al₂O₃) exhibited much higher NO oxidation activity than Pd catalyst [28,56].

4. Conclusions

The oxidation of propane, iso-pentane and propylene over aged Pt/Al₂O₃, Pd/Al₂O₃ and Pt–Pd/Al₂O₃ catalysts was investigated under near-stoichiometric and fully lean conditions. The oxidation states of the catalysts were characterized with XRD, XANES and STEM before and after the reaction. Under both slightly lean and slightly rich conditions, the Pt/Al₂O₃ catalyst was the most active for propane oxidation; for propylene oxidation, however, the Pd/Al₂O₃ catalyst exhibited the highest activity, followed by the Pt–Pd/Al₂O₃ and Pt/Al₂O₃ catalysts. When the oxygen concentration in the feed increased from 1 to 10% (characteristic of lean gasoline engine exhaust), the activity of the Pt/Al₂O₃ catalyst for propane oxidation drastically decreased due to oxygen poisoning of the Pt surface, reaching only 50% conversion at ~500 °C. On the other hand, the activity for iso-pentane oxidation was affected only to a relatively small extent by the high oxygen concentration and thus the same activity order among the catalysts (Pt > Pt–Pd > Pd) was observed under both the slightly lean and fully lean conditions. The propylene oxidation activity was greatly enhanced over all three catalysts in the presence of excess oxygen in the fully lean feed. These results indicate that both hydrocarbon type and oxygen concentration level are important factors determining the relative oxidation activities of the various noble metal catalysts. Relatively small beneficial effects of Pt–Pd alloying were observed during iso-pentane oxidation at low temperatures under the near-stoichiometric conditions and during propane oxidation at high temperatures under the fully lean condition. However, alloy formation was found to be detrimental for the propane oxidation under the slightly lean condition.

Acknowledgements

This study was financially supported by General Motors Corporation. The Ministry of Science, ICT, and Future Planning (MSIP) and the Pohang University of Science and Technology (POSTECH) supported the XAFS experiments at PLS-II.

Appendix A. Supplementary data

Supplementary material related to this article can be found, in the online version, at doi:<https://doi.org/10.1016/j.apcatb.2019.04.001>.

References

- [1] H.S. Gandhi, G.W. Graham, R.W. McCabe, Automotive exhaust catalysis, *J. Catal.* 216 (2003) 433–442.
- [2] M. Zheng, U. Asad, G.T. Reader, Y.Y. Tan, M.P. Wang, Energy efficiency improvement strategies for a diesel engine in low-temperature combustion, *Int. J. Energy Res.* 33 (2009) 8–28.
- [3] S. Chu, A. Majumdar, Opportunities and challenges for a sustainable energy future, *Nature* 488 (2012) 294.
- [4] K.L. Olson, R.M. Sinkevitch, T.M. Sloane, Speciation and quantitation of hydrocarbons in gasoline-engine exhaust, *J. Chromatogr. Sci.* 30 (1992) 500–508.
- [5] C. Henry, S. Kroll, V. Premnath, I. Smith, P. Morgan, I. Khalek, Detailed Characterization of Criteria Pollutant Emissions From D-EGR[®] Light Duty Vehicle, SAE Technical Paper, 2016-01-1006, (2016), <https://doi.org/10.4271/2016-4201-1006>.
- [6] Y.F.Y. Yao, Oxidation of alkanes over noble-metal catalysts, *Ind. Eng. Chem. Prod. Res. Dev.* 19 (1980) 293–298.
- [7] Y.F.Y. Yao, The oxidation of CO and hydrocarbons over noble-metal catalysts, *J. Catal.* 87 (1984) 152–162.
- [8] A.B. Kooh, W.J. Han, R.G. Lee, R.F. Hicks, Effect of catalyst structure and carbon deposition on heptane oxidation over supported platinum and palladium, *J. Catal.* 130 (1991) 374–391.
- [9] C.H. Kim, M. Schmid, S.J. Schmieg, J. Tan, W. Li, The Effect of Pt–Pd Ratio on Oxidation Catalysts Under Simulated Diesel Exhaust, SAE Technical Paper, 2011-01-1134, (2011), <https://doi.org/10.4271/2011-4201-1134>.
- [10] A. Morlang, U. Neuhausen, K.V. Klementiev, F.W. Schutze, G. Miehe, H. Fuess, E.S. Lox, Bimetallic Pt/Pd diesel oxidation catalysts – structural characterisation and catalytic behaviour, *Appl. Catal. B* 60 (2005) 191–199.
- [11] H.F. Xiong, E. Peterson, G.S. Qi, A.K. Datye, Trapping mobile Pt species by PdO in diesel oxidation catalysts: smaller is better, *Catal. Today* 272 (2016) 80–86.
- [12] N.M. Kinnunen, J.T. Hirvi, M. Suvanto, T.A. Pakkanen, Methane combustion activity of Pd–PdOx–Pt/Al₂O₃ catalyst: the role of platinum promoter, *J. Mol. Catal. A Chem.* 356 (2012) 20–28.
- [13] R. Strobel, J.-D. Grunwaldt, A. Camenzind, S.E. Pratsinis, A. Baiker, Flame-made alumina supported Pd–Pt nanoparticles: structural properties and catalytic behavior in methane combustion, *Catal. Lett.* 104 (2005) 9–16.
- [14] I.A. Resitoglu, K. Altinisik, A. Keskin, The pollutant emissions from diesel-engine vehicles and exhaust aftertreatment systems, *Clean Technol. Environ. Policy* 17 (2015) 15–27.
- [15] M.J. Patterson, D.E. Angove, N.W. Cant, The effect of carbon monoxide on the oxidation of four C6 to C8 hydrocarbons over platinum, palladium and rhodium, *Appl. Catal. B* 26 (2000) 47–57.
- [16] S.R. Katore, P.M. Laing, Hydrogen in diesel exhaust: effect on diesel oxidation catalyst flow reactor experiments and model predictions, *SAE Int. J. Fuels Lubr.* 2 (1) (2009) 605–611, <https://doi.org/10.4271/2009-01-1268>.
- [17] N. Sadokhina, G. Smedler, U. Nylen, M. Olofsson, L. Olsson, The influence of gas composition on Pd-based catalyst activity in methane oxidation – inhibition and promotion by NO, *Appl. Catal. B* 200 (2017) 351–360.
- [18] R. Caporali, S. Chansai, R. Burch, J.J. Delgado, A. Goguet, C. Hardacre, L. Mantarosi, D. Thompsett, Critical role of water in the direct oxidation of CO and hydrocarbons in diesel exhaust after treatment catalysis, *Appl. Catal. B* 147 (2014) 764–769.
- [19] Y.-H. Chin, M. García-Diéguez, E. Iglesia, Dynamics and Thermodynamics of Pd–PdO phase transitions: effects of Pd cluster size and kinetic implications for catalytic methane combustion, *J. Phys. Chem. C* 120 (2016) 1446–1460.
- [20] M. Haneda, K. Suzuki, M. Sasaki, H. Hamada, M. Ozawa, Catalytic performance of bimetallic PtPd/Al₂O₃ for diesel hydrocarbon oxidation and its implementation by acidic additives, *Appl. Catal. A Gen.* 475 (2014) 109–115.
- [21] G.S. Bugosh, V.G. Easterling, I.A. Rusakova, M.P. Harold, Anomalous steady-state and spatio-temporal features of methane oxidation on Pt/Pd/Al₂O₃ monolith spanning lean and rich conditions, *Appl. Catal. B* 165 (2015) 68–78.
- [22] S.B. Kang, S.J. Han, S.B. Nam, I.S. Nam, B.K. Cho, C.H. Kim, S.H. Oh, Activity function describing the effect of Pd loading on the catalytic performance of modern commercial TWC, *Chem. Eng. J.* 207 (2012) 117–121.
- [23] C.C. Webb, B.B. Bykowski, Development of a Methodology to Separate Thermal From Oil Aging of a Catalyst Using a Gasoline-fueled Burner System, SAE Technical Paper, 2003-01-0663, (2003), <https://doi.org/10.4271/2003-4201-0663>.
- [24] S.B. Kang, M. Hazlett, V. Balakotaiah, C. Kalamaras, W. Epling, Effect of Pt:Pd ratio on CO and hydrocarbon oxidation, *Appl. Catal. B* 223 (2018) 67–75.
- [25] S.B. Kang, I.S. Nam, B.K. Cho, C.H. Kim, S.H. Oh, Universal activity function for predicting performance of Pd-based TWC as function of Pd loading and catalyst mileage, *Chem. Eng. J.* 259 (2015) 519–533.
- [26] J.R. González-Velasco, J.A. Botas, J.A. González-Marcos, M.A. Gutiérrez-Ortiz, Influence of water and hydrocarbon processed in feedstream on the three-way behaviour of platinum-alumina catalysts, *Appl. Catal. B* 12 (1997) 61–79.
- [27] J.H. Baik, H.J. Kwon, Y.T. Kwon, I.S. Nam, S.H. Oh, Effects of catalyst aging on the activity and selectivity of commercial three-way catalysts, *Top. Catal.* 42–43 (2007) 337–340.
- [28] O.K. Ezekoye, A.R. Drews, H.W. Jen, R.J. Kudla, R.W. McCabe, M. Sharma, J.Y. Howe, L.F. Allard, G.W. Graham, X.Q. Pan, Characterization of alumina-supported Pt and Pt–Pd NO oxidation catalysts with advanced electron microscopy, *J. Catal.* 280 (2011) 125–136.
- [29] X.Y. Chen, Y.S. Cheng, C.Y. Seo, J.W. Schwank, R.W. McCabe, Aging, re-dispersion, and catalytic oxidation characteristics of model Pd/Al₂O₃ automotive three-way catalysts, *Appl. Catal. B* 163 (2015) 499–509.
- [30] M. Kaneeda, H. Iizuka, T. Hiratsuka, N. Shinotsuka, M. Arai, Improvement of thermal stability of NO oxidation Pt/Al₂O₃ catalyst by addition of Pd, *Appl. Catal. B* 90 (2009) 564–569.
- [31] S.B. Simonsen, I. Chorkendorff, S. Dahl, M. Skoglundh, J. Sehested, S. Helveg, Direct observations of oxygen-induced platinum nanoparticle ripening studied by in situ TEM, *J. Am. Chem. Soc.* 132 (2010) 7968–7975.
- [32] H. Shinjoh, H. Muraki, Y. Fujitani, Effect of severe thermal aging on noble metal catalysts, *Stud. Surf. Sci. Catal.* 71 (1991) 617–628.
- [33] J. Lee, Y. Ryou, J. Kim, X. Chan, T.J. Kim, D.H. Kim, Influence of the defect concentration of Ceria on the Pt dispersion and the CO oxidation activity of Pt/CeO₂, *J. Phys. Chem. C* 122 (2018) 4972–4983.
- [34] T.C. Chang, J.J. Chen, C.T. Yeh, Temperature-programmed reduction and temperature-resolved sorption studies of strong metal-support interaction in supported palladium catalysts, *J. Catal.* 96 (1985) 51–57.
- [35] L.F. Chen, G. González, J.A. Wang, L.E. Noreña, A. Toledo, S. Castillo, M. Morán-Pineda, Surfactant-controlled synthesis of Pd/CeO₂ 6Zr_{0.4}O₂ catalyst for NO reduction by CO with excess oxygen, *Appl. Surf. Sci.* 243 (2005) 319–328.
- [36] A. Boubnov, S. Dahl, E. Johnson, A.P. Molina, S.B. Simonsen, F.M. Cano, S. Helveg, L.J. Lemus-Yegres, J.-D. Grunwaldt, Structure–activity relationships of Pt/Al₂O₃ catalysts for CO and NO oxidation at diesel exhaust conditions, *Appl. Catal. B* 126 (2012) 315–325.
- [37] J. Singh, E.M. Alayon, M. Tromp, O.V. Safonova, P. Glatzel, M. Nachttegaal, R. Frahm, J.A. van Bokhoven, Generating highly active partially oxidized platinum during oxidation of carbon monoxide over Pt/Al₂O₃: in situ, time-resolved, and high-energy-resolution X-ray absorption spectroscopy, *Angew. Chem. Int. Ed. Engl.* 47 (2008) 9260–9264.
- [38] R. Burch, D.J. Crittle, M.J. Hayes, C–H bond activation in hydrocarbon oxidation on heterogeneous catalysts, *Catal. Today* 47 (1999) 229–234.
- [39] M. Skoglundh, L.O. Löwendahl, J.E. Otterstedt, Combinations of platinum and palladium on alumina supports as oxidation catalysts, *Appl. Catal.* 77 (1991) 9–20.
- [40] F. Diehl, J. Barbier Jr., D. Duprez, I. Guibard, G. Mabilon, Catalytic oxidation of heavy hydrocarbons over Pt/Al₂O₃. Influence of the structure of the molecule on its

- reactivity, *Appl. Catal. B: Environ.* 95 (2010) 217–227.
- [41] N. Cant, Catalytic oxidation II. Silica supported noble metals for the oxidation of ethylene and propylene, *J. Catal.* 16 (1970) 220–231.
- [42] M.J. Hazlett, W.S. Epling, Spatially resolving CO and C₃H₆ oxidation reactions in a Pt/Al₂O₃ model oxidation catalyst, *Catal. Today* 267 (2016) 157–166.
- [43] M.J. Hazlett, M. Moses-Debusk, J.E. Parks, L.F. Allard, W.S. Epling, Kinetic and mechanistic study of bimetallic Pt–Pd/Al₂O₃ catalysts for CO and C₃H₆ oxidation, *Appl. Catal. B* 202 (2017) 404–417.
- [44] Z.Z. Yang, J. Li, H.L. Zhang, Y. Yang, M.C. Gong, Y.Q. Chen, Size-dependent CO and propylene oxidation activities of platinum nanoparticles on the monolithic Pt/TiO₂-YOx diesel oxidation catalyst under simulative diesel exhaust conditions, *Catal. Sci. Technol.* 5 (2015) 2358–2365.
- [45] M.Q. Shen, G.X. Wei, H.M. Yang, J. Wang, X.Q. Wang, Different selections of active sites for CO, C₃H₆, and C₁₀H₂₂ oxidation on Pd/CeO₂ catalysts, *Fuel* 103 (2013) 869–875.
- [46] C. Campbell, D. Foyt, J. White, Oxygen penetration into the bulk of palladium, *J. Phys. Chem.* 81 (1977) 491–494.
- [47] T. Schalow, B. Brandt, D.E. Starr, M. Laurin, S.K. Shaikhutdinov, S. Schauermaun, J. Libuda, H.J. Freund, Size-dependent oxidation mechanism of supported Pd nanoparticles, *Angew. Chem. Int. Ed. Engl.* 45 (2006) 3693–3697.
- [48] P. Castellazzi, G. Groppi, P. Forzatti, Effect of Pt/Pd ratio on catalytic activity and redox behavior of bimetallic Pt–Pd/Al₂O₃ catalysts for CH₄ combustion, *Appl. Catal. B* 95 (2010) 303–311.
- [49] H. Shinjoh, H. Muraki, Y. Fujitani, Periodic operation effects in propane and propylene oxidation over noble metal catalysts, *Appl. Catal.* 49 (1989) 195–204.
- [50] K. Persson, K. Jansson, S. Jaras, Characterisation and microstructure of Pd and bimetallic Pd–Pt catalysts during methane oxidation, *J. Catal.* 245 (2007) 401–414.
- [51] R. Burch, F.J. Urbano, P.K. Loader, Methane combustion over palladium catalysts: the effect of carbon dioxide and water on activity, *Appl. Catal. A Gen.* 123 (1995) 173–184.
- [52] C. Carrillo, A. DeLaRiva, H.F. Xiong, E.J. Peterson, M.N. Spilde, D. Kunwar, R.S. Goeke, M. Wiebenga, S.H. Oh, G.S. Qi, S.R. Challa, A.K. Datye, Regenerative trapping: how Pd improves the durability of Pt diesel oxidation catalysts, *Appl. Catal. B* 218 (2017) 581–590.
- [53] L. Kiwi-Minsker, I. Yuranov, E. Slavinskaia, V. Zaikovskii, A. Renken, Pt and Pd supported on glass fibers as effective combustion catalysts, *Catal. Today* 59 (2000) 61–68.
- [54] A. Schwartz, L.L. Holbrook, H. Wise, Catalytic oxidation studies with platinum and palladium, *J. Catal.* 21 (1971) 199–207.
- [55] P.D. Szuromi, J.R. Engstrom, W.H. Weinberg, Adsorption and reaction of *n*-alkanes on the platinum(110)-(1. times. 2) surface, *J. Phys. Chem.* 89 (1985) 2497–2502.
- [56] S. Salasc, M. Skoglundh, E. Fridell, A comparison between Pt and Pd in NO_x storage catalysts, *Appl. Catal. B* 36 (2002) 145–160.